Elastic and Magnetic Dynamics of Nanomagnet-Ordered Arrays Impulsively Excited by Subpicosecond Laser Pulses

A. Comin,[1] C. Giannetti,[1] G. Samoggia,[2] P. Vavassori,[3] D. Grando,[4] P. Colombi,[5] E. Bontempi,[5] L. E. Depero,[5] V. Metlushko,[6] B. Ilic,[7] and F. Parmigiani[8,*]

[1]*Sincrotrone Trieste, I-34012 Basovizza, Trieste, Italy, and Dipartimento di Matematica e Fisica, Università Cattolica del Sacro Cuore, I-25121 Brescia, Italy*
[2]*Dipartimento di Fisica "A. Volta," Università degli Studi di Pavia, I-27100 Pavia, Italy*
[3]*CNR-INFM CRS S3 and Dipartimento di Fisica, Università di Ferrara, I-44100 Ferrara, Italy*
[4]*Dipartimento di Elettronica, Università degli Studi di Pavia, I-27100 Pavia, Italy*
[5]*Laboratorio di Chimica per le Tecnologie, Università degli Studi di Brescia, I-25123 Brescia, Italy*
[6]*Department of Electrical and Computer Engineering, University of Illinois at Chicago, Chicago, Illinois 60607, USA*
[7]*Cornell Nanofabrication Facility, School of Applied and Engineering Physics, Cornell University, Ithaca, New York 14853, USA*
[8]*Dipartimento di Fisica, Università degli Studi di Trieste, I-34127 Trieste, Italy, and Sincrotrone Trieste, I-34012 Basovizza, Trieste, Italy*

(Received 23 September 2005; revised manuscript received 27 April 2006; published 20 November 2006)

This Letter reports on the first observation of elastic and magnetic dynamics of ordered arrays of permalloy nanodots excited by low-intensity 120 fs light pulses. The first order of the diffraction pattern, generated by the probe beam in a pump-probe configuration, is used for time-resolved reflectivity and time-resolved magneto-optical Kerr effect measurements. The nonadiabatical absorption of the pump triggers an acoustic standing wave, detected by the reflected probe signal, with a frequency related to the array wave vector. Instead, the magneto-optical signal exhibits, on the nanosecond time scale, the signature of the heat-exchange diffusion processes. In addition, a clear oscillation of the magnetic signal, at a frequency close to the frequency of the acoustic wave, is unambiguously detected. Finally, the interplay between the elastic and magnetic dynamics is analyzed and interpreted.

DOI: 10.1103/PhysRevLett.97.217201 PACS numbers: 75.75.+a, 75.80.+q, 78.47.+p

Nowadays, the study of the thermodynamic and magnetic properties of submicrometric solids represents one of the most important technological and scientific achievements [1–5]. However, up to now, the possibility of measuring mechanical and magnetic properties of nanoscaled solids in nonequilibrium conditions after excitation with short coherent light pulses has not been exploited.

In this Letter, we demonstrate that it is possible to excite acoustic standing waves in square arrays of permalloy nanodots deposited on a Si substrate, employing ~120 fs laser pulses from a titanium-sapphire (Ti:sapphire) oscillator. The acoustic surface waves can be modeled as mixed longitudinal and transverse modes, with wave vectors given by the inverse of the array period and frequencies related to the elastic properties of the substrate. We also show that it is possible to follow the relaxation of the magnetization during the heat-exchange process with the silicon substrate. Finally, oscillations in the magnetic signal at the same frequency of the acoustic waves are detected and discussed.

Exploiting the knowledge that time-resolved reflectivity measurements and magneto-optical Kerr effect (MOKE) can be used to detect the strains [6,7] and the magnetization of thin films [8,9], we have designed and applied a time-resolved magneto-optical Kerr effect (TR-MOKE) apparatus to measure the dynamics of elastic and magnetic properties of permalloy (Fe-Ni alloy) nanosized systems. The present experiment takes advantage of the fact that, for ordered arrays of metallic nanostructures deposited on a silicon substrate, it is possible to analyze the diffraction pattern, thus improving the signal to noise ratio. In this configuration, the pump pulse impulsively heats the metallic nanostructure (the thermalization between the excited electrons and the phonon gas is completed in less than one picosecond), inducing a nonadiabatic thermal expansion which triggers acoustic standing waves in the system.

Different sets of cylindrical nanodots, with a nominal composition of $Fe_{20}Ni_{80}$ and arranged on ordered square lattices, have been prepared using electron-beam lithography and lift-off techniques on a silicon substrate oriented along the (100) direction. The array period, the dot thickness, and the diameters have been carefully measured by AFM (atomic force microscopy) and grazing-angle x-ray reflectivity. Nanodot arrays with nominal periods of 600, 800, 1000, and 2100 nm and thicknesses of 30 nm have been studied with time-resolved reflectivity spectroscopy. The diameter of the dots, as measured by AFM, is half of the array period. A sample with a period of 1000 nm and a dot diameter of 600 nm was used for the TR-MOKE measurements.

A conventional pump-probe setup [10], reported in Fig. 1, based on a 76 MHz repetition rate Ti:sapphire oscillator operating at a central wavelength of $\simeq$800 nm, is used to detect the ellipticity and intensity of the first-order diffracted beam, which yields to a significant improvement of the signal to noise ratio, as analyzed in Ref. [11].

The pulse duration is ~120 fs. The energy of the pump pulse is ≲10 nJ, while less than 1 nJ is used for the probe. To optimize the optical signal to noise ratio, we set the spot sizes of the pump and probe beams to 40 and 30 μm, respectively, and adopt a double lock-in technique [12]. In this configuration, a photoelastic modulator (PEM) varies the polarization of the probe at 50 kHz. The signal is filtered by the lock-in amplifier operating at 50 or 100 kHz, to obtain the ellipticity and the rotation. The output signal is then processed by a second lock-in amplifier referenced to a 150 Hz chopper on the pump beam. The measurements have been taken in the longitudinal geometry (magnetic field H parallel to the sample surface and to the plane of incidence of light), as shown in Fig. 1. In this configuration, the rotation and ellipticity of the first-order diffracted beam are accessible on the picosecond time scale and directly related to the magnetization of the system [13]. On the bottom right of the left inset in Fig. 1, the ellipticity signal detected by the first lock-in amplifier is reported as a function of the applied magnetic field for the 1000 nm-period sample. The shape of the hysteresis cycle is reproduced by micromagnetic simulations, which show the formation of a magnetic vortex structure at $H \simeq 0$, where a drop in the hysteresis loop is observed. The subsequent smooth approach to saturation corresponds to the vortex core displacement as the external field is increased (in modulus) until the vortex state finally annihilates and a single-domain configuration is established [14].

The inset on the right in Fig. 2 displays the variation of the intensity of the first-order diffracted signal $\Delta I_{1D}/I_{1D}$ from the 1000 nm-period sample. During the first few femtoseconds, the signal quickly rises and follows the autocorrelation trace of the pump pulse, then exponentially decays, with a time constant of hundreds of femtoseconds. This feature can be attributed to the excitation of a nonequilibrium electron population which is rapidly thermalizing with the phonon gas. On the picosecond time scale, one recognizes a pronounced oscillation in the diffracted intensity with a period of ~220 ps. We repeated the measurements of the transient reflectivity signal for samples with different array periods D (see Fig. 2). The relationship between the measured oscillation frequencies and the inverse array period is linear, as clearly shown in the left inset in Fig. 2.

As a consequence of the elastic interaction between the dots and the substrate, the pump excitation induces a longitudinal stress in the silicon with a periodicity D given by the array period, triggering a surface acoustic wave (SAW) with wave vector $q = 2\pi/D$. By changing the array periodicity, it is possible to excite SAWs in the substrate with different wave vectors q. The frequency of the SAW is $\omega = \xi c_t q$ [15], where c_t is the transverse sound velocity and the coefficient $\xi < 1$ depends only on the Poisson ratio σ of the material ($\sigma \simeq 0.27$ and $\xi \simeq 0.92$ for silicon [15,16]). The linear fit to data (dashed line in the left inset in Fig. 2) gives $c_t \simeq 5100 \pm 300$ m/s. From this value, it is possible to obtain the Young modulus $Y = 2\rho(1+\sigma)c_t^2 \simeq 150 \pm 20$ GPa ($\rho = 2340$ kg/m^3 is the silicon density), a result compatible with the Young modulus $Y = 130$ GPa of Si(100) [16]. To further confirm the attribution of the measured oscillations to a SAW in silicon and disentangle the contribution of the variation of the period of the array from the variation of the dot diameter, we prepared a new set of samples with constant periodicity ($D = 1$ μm) and thickness ($h = 50$ nm) and different dot diameters ($2a = 320$, 400, and 790 nm). In this case, only a slight shift of the frequency ($\Delta\omega/\omega \simeq 6\%$) is evidenced. This is the signature of an elastic coupling between the

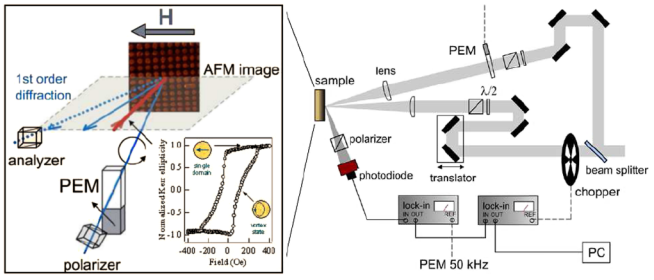

FIG. 1 (color online). Schematic of the time-resolved MOKE setup. In the left-hand panel are shown an AFM image of the sample and the hysteresis cycle obtained in the longitudinal Kerr configuration for the 1000 nm-period sample.

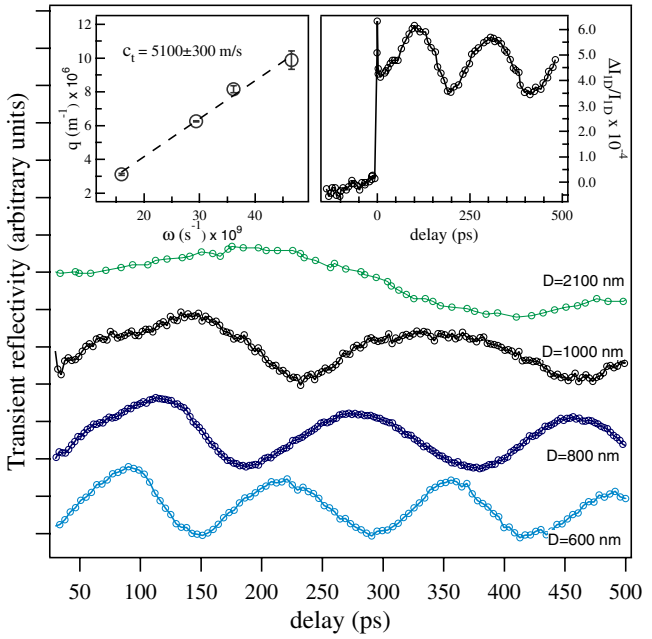

FIG. 2 (color online). Time-resolved reflectivity on the first-order diffraction from ordered arrays of permalloy nanodots. In the right inset, the detected signal on the full temporal scale is shown for the 1000 nm-period sample. In the figure, the normalized slow oscillating component is shown for samples with different array periods D. In the left inset, the wave vector as a function of the measured oscillation frequency is reported. The dashed line is a linear fit to the data.

substrate and the metallic array, resulting in a slight renormalization of the surface wave velocity as a function of the filling factor, i.e., the ratio between the dot surface and the unit cell [17]. The excitation of SAWs in a substrate via laser-induced heating of a deposited metallic structure was already investigated in the case of 1D grating constituted by thin gold stripes (a nonmagnetic material) on a silicon substrate [18], indicating that this phenomenon is independent on the material deposited on the substrate.

The magnetization dynamics has been studied using the time-resolved magneto-optical setup described in Fig. 1. In the longitudinal configuration, the variation of the Kerr signal δI_{Kerr}, induced by the pump excitation, is given by [19]

$$\delta I_{\mathrm{Kerr}} = \delta R + \delta M = \delta R + K J_1(\Delta)\delta\,\mathrm{Im}(f_1 r_{\mathrm{pp}}^{*} f_1^{m} r_{\mathrm{ps}}^{m}), \quad (1)$$

where δR is a nonmagnetic contribution arising from possible misalignments of the optical components and from the variation of the temperature of the sample at the pump modulation frequency (150 Hz); therefore, δR is proportional to the reflectivity signal. The second term δM is proportional to the Kerr coefficient K, to the Bessel function $J_1(\Delta)$ (Δ is the amplitude of the PEM modulation, set to 2.405 in the present case), and to the variation of the reflectivity, $f_1 = \int_S e^{-i\mathbf{r}\cdot\mathbf{q}} ds$ (S is the dot surface) being the first-order geometric form factor, $f_1^m = \int_S m_{\parallel} e^{-i\mathbf{r}\cdot\mathbf{q}} ds \simeq m_{\parallel} f_1$ the magnetic form factor assuming $m_{\parallel}$ (the magnetization component in the incidence plane) constant in the dot volume, and r_{pp}^{*} and r_{ps}^{m} the nonmagnetic and magnetic parts of the tensorial reflectivity coefficient, respectively.

The pump-induced variation of the hysteresis cycles (δI_{Kerr} vs H) has been recorded, as a function of the delay between the pump and probe pulses, for the 1000 nm dot diameter sample. The as-measured transient cycles exhibit an offset due to the δR contributions. We measured several transient hysteresis cycles at different delay times between -100 and 520 ps. To ease the comparison, we report the transient hysteresis cycles for 12, 280, and 520 ps delay times, after the graphical subtraction of the offset (see left inset in Fig. 3). As expected, since δM is proportional to $m_{\parallel}$ [see Eq. (1)], the shape of the measured variation of the hysteresis cycles is similar to the static magnetic hysteresis cycle (see Fig. 1).

In order to gain information on the magnetization dynamics, we evaluated the difference of the as-measured (with the offset) δI_{Kerr} at $+H$ and $-H$, correspondent to opposite $m_{\parallel}$ values. This procedure is based on the fact that only the δM contribution changes sign upon inversion of the magnetization, whereas δR is unchanged [10]. Therefore, the net magnetic signal variation δM is given by

$$\delta M = \tfrac{1}{2}[\delta I_{\mathrm{Kerr}}(H, m_{\parallel}) - \delta I_{\mathrm{Kerr}}(-H, -m_{\parallel})]. \quad (2)$$

Conversely, δR is given by

$$\delta R = \tfrac{1}{2}[\delta I_{\mathrm{Kerr}}(H, m_{\parallel}) + \delta I_{\mathrm{Kerr}}(-H, -m_{\parallel})]; \quad (3)$$

therefore, δR represents the offset detected in the transient hysteresis cycles. In the right inset in Fig. 3 (black circles, left axis), the δR signal, obtained from Eq. (3), is reported as a function of the pump and probe delay. It is important to note that this signal exhibits oscillations at the same frequency of the time-resolved reflectivity (see Fig. 2), in agreement with the nonmagnetic nature of such a contribution.

In Fig. 3, the normalized magnetic dynamics $\delta M/M$, obtained at saturation, is reported. A very fast demagnetization is evident. The origin of this magneto-optical effect is a long-debated question [8,9] that, however, overtakes the scope of the present Letter. The following slow magnetization recovery, with a time constant of hundreds of picoseconds, is related to the heat exchange between the excited nanodots, whose temperature impulsively increases of $\simeq 30$ K [20], and the silicon substrate. This result demonstrates that it is possible to directly measure the magnetization dynamics during the heat-exchange process between a nanosystem and the substrate.

In the right inset in Fig. 3, the residual of the fit to the magnetization dynamics at saturation is shown (dots, right axis). An oscillation of $\delta M/M$ of the order of 10^{-4} and quasi-in-phase with the reflectivity variation is evidenced. Neglecting the time dependence of the reflectivity coefficients, the relative variation of the magnetic signal is $\delta M/M \simeq \delta m_{\parallel}/m_{\parallel} + \delta f_1^2/f_1^2$. As a consequence, the mea-

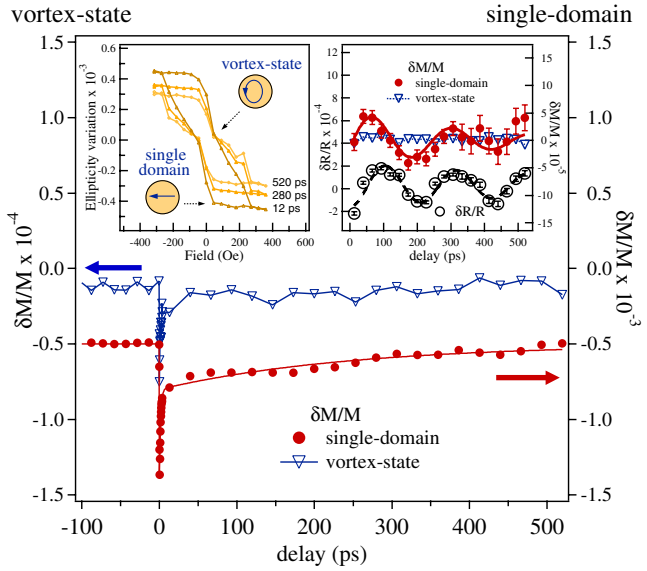

FIG. 3 (color online). The time-resolved magnetization dynamics ($\delta M/M$) in the vortex phase (triangles, left axis) or in the single-domain configuration (dots, right axis) of the 1000 nm-period sample. The solid line is the best fit of the data to two exponential decays convoluted with a Gaussian representing the experimental temporal resolution. The left inset shows the variation of magnetic hysteresis cycles, taken at three delays between the pump and probe pulses. The inset at right displays the residual of the fit of the magnetization dynamics (right axis) and the offsets of the transient hysteresis cycles (black empty circles, left axis).

sured oscillation could be attributed to the time-dependent modulation of the f_1 form factor or to a change of the magnetization vector arising from the magnetoelastic interaction. The magnetoelastic coupling is related to a bilinear dependence of the thermodynamic potential per unit volume on the magnetization components: $g(\mathbf{M}, \sigma) = \sigma_{ij}\lambda_{ijkl}M_kM_l$ [21], where σ_{ij} is the stress tensor and λ_{ijkl} is the magnetostriction coefficient, depending on the relative Fe-Ni stoichiometry [22]. Unfortunately, in the present case, both of these processes equally contribute to the variation of the magneto-optical signal, and they cannot be easily disentangled [23]. Nonetheless, we underline that the best fit to the magneto-optical oscillation, reported in the right inset in Fig. 3 (solid line), is obtained with a damped sinlike function with a period of $\simeq 240$ ps, whereas the reflectivity oscillation (black circles) is fitted with a (1-cos)-like function (black dashed line) with a period of $\simeq 220$ ps. A careful analysis of the $\delta M/M$ dynamics showed no dependence of the oscillation frequency, phase, and amplitude on the external field H as it is varied in the range 360–90 Oe (below 90 Oe, the vortex state nucleates and M drops to zero). This rules out the possibility that the observed oscillation is a resonance triggered directly by the high frequency components of the deltalike excitation.

These results are confirmed by the measurements of the variation of the Kerr signal versus the delay time at $m_{\parallel} = 0$. When approaching $m_{\parallel} = 0$, the δM signal is vanishing and the variation of the magnetization is not detectable anymore, although the relaxation time driven by the dot-substrate heat exchange should be the same for any $m_{\parallel}$. As a consequence, at $m_{\parallel} = 0$, only a complete subtraction of the δR contributions [see Eq. (1)] will give a variation of the magnetization close to zero, i.e., $\delta M = 1/2[\delta I_{\mathrm{Kerr}}(H, 0) - \delta I_{\mathrm{Kerr}}(-H, 0)] \simeq 0$. This is consistent with the $\delta M/M$ measurements, at $m_{\parallel} = 0$, reported in Fig. 3 (triangles, left axis) and in the right inset in Fig. 3 (triangles, right axis). At this light, the variation of the Kerr signal observed, after the subtraction of δR, can be unambiguously related to the magnetization dynamics.

This work was supported by the Italian Ministero dell'Istruzione, Università e Ricerca (MIUR) under Contracts No. FIRB-RBNE0155X7 and No. PRIN2004027288 and by the project Nano&Nano of the Ferrara State University.

*Electronic address: fulvio@dmf.unicatt.it

[1] R. Cowburn, D. Koltsov, A. Adeyeye, M. Welland, and D. Tricker, Phys. Rev. Lett. **83**, 1042 (1999).
[2] T. Shinjo, T. Okuno, R. Hassdorf, K. Shigeto, and T. Ono, Science **289**, 930 (2000).
[3] W. K. Hiebert, A. Stankiewicz, and M. R. Freeman, Phys. Rev. Lett. **79**, 1134 (1997).
[4] M. Buess, R. Höllinger, T. Haug, K. Perzlmaier, U. Krey, D. Pescia, M. R. Scheinfein, D. Weiss, and C. H. Back, Phys. Rev. Lett. **93**, 077207 (2004).
[5] M. van Kampen, C. Jozsa, J. Kohlepp, P. LeClair, L. Lagae, W. de Jonge, and B. Koopmans, Phys. Rev. Lett. **88**, 227201 (2002).
[6] C. Thomsen, H. T. Grahn, J. J. Maris, and J. Tauc, Phys. Rev. B **34**, 4129 (1986).
[7] I. Bozovic, M. Schneider, Y. Xu, R. Sobolewski, Y. H. Ren, G. Lpke, J. Demsar, A. J. Taylor, and M. Onellion, Phys. Rev. B **69**, 132503 (2004).
[8] E. Beaurepaire, J. Merle, A. Daunois, and J. Bigot, Phys. Rev. Lett. **76**, 4250 (1996).
[9] B. Koopmans, M. van Kampen, J. T. Kohlhepp, and W. J. M. de Jonge, Phys. Rev. Lett. **85**, 844 (2000).
[10] A. Comin, M. Rossi, C. Mozzati, F. Parmigiani, and G. Banfi, Solid State Commun. **129**, 227 (2004).
[11] In the reflected signal, the contribution of the substrate with respect to the dots is proportional to the ratio between the area of the substrate within the unit cell and that of the single magnetic dot, viz. $[(4a)^2 - \pi a^2]/\pi a^2 \simeq 4$. In the diffracted signal, the contribution of the substrate is proportional to πa^2, leading to an improvement of the signal to noise ratio of ~ 4.
[12] B. Koopmans, M. van Kampen, J. T. Kohlhepp, and W. J. M. de Jonge, J. Appl. Phys. **87**, 5070 (2000).
[13] B. Koopmans, M. van Kampen, and W. J. M. de Jonge, J. Phys. Condens. Matter **15**, S723 (2003).
[14] M. Grimsditch, P. Vavassori, V. Novosad, V. Metlushko, H. Shima, Y. Otani, and K. Fukamichi, Phys. Rev. B **65**, 172419 (2002).
[15] L. Landau and E. Lifshitz, *Theory of Elasticity* (Butterworth-Heinemann, Oxford, 1986).
[16] J. Wortman and R. Evans, J. Appl. Phys. **36**, 153 (1965).
[17] Since the physics of the coupling between the surface wave and the metallic array is not the main goal of this Letter, we will discuss in detail these new data in a different context.
[18] D. Hurley and K. Telschow, Phys. Rev. B **66**, 153301 (2002).
[19] M. Grimsditch and P. Vavassori, J. Phys. Condens. Matter **16**, R275 (2004).
[20] The temperature variation has been estimated by solving the heat equation in the case of a 30 nm thick permalloy film excited by 10 nJ laser pulses.
[21] M. Schlenker and É. du Trémolet de Lacheisserie, in *Magnetism, Fundamentals*, edited by É. du Trémolet de Lacheisserie, D. Gignoux, and M. Schlenker (Springer, New York, 2003).
[22] O. Buckley and L. McKeehan, Phys. Rev. **26**, 261 (1925).
[23] Both the variation of the f_1 form factor of an oscillating flat disk and the magnitude variation of the magnetization of a disk subjected to a radial stress $\sigma_{rr} = Y\delta r/r$ relative to the radius variation $\delta r/r$ and with an isotropic magnetostriction coefficient $\lambda \simeq 1 \times 10^{-7}$ are estimated to be of the order of 10^{-4}, compatible with the amplitude of the measured oscillation.